Effect of irradiation with heavy Xe^{22+} ions with energies of 165-230 MeV on change in optical characteristics of ZrO_2 ceramic

Ivanov I.A.[1,2], M.Alin[1], Koloberdin M.V.[2], Sapar A.[1,2], Kurakhmedov A.E.[2], A.L. Kozlovskiy[1,2*], M.V. Zdorovets[1,2,3], Uglov V.V.[4]

[1]*L.N. Gumilyov Eurasian National University, Nur-Sultan, Kazakhstan*
[2]*The Institute of Nuclear Physics of Republic of Kazakhstan, Almaty, Kazakhstan*
[3]*Ural Federal University, Yekaterinburg, Russia*
[4]*Belarusian State University, Minsk, Belarus*
*E-mail: kozlovskiy.a@inp.kz

Abstract

The aim of this work is to study the effect of irradiation with heavy Xe^{22+} ions with energies of 165 MeV, 200 MeV, and 230 MeV on the change in the optical properties of ZrO_2 ceramic. The choice of ion energies, as well as irradiation fluences of 10^{13}-10^{14} ion/cm^2, is primarily due to the possibility of simulating radiation damage in ceramics that occurs when overlapping damaged areas in the material, comparable to damage from fission fragments of uranium nuclei in an atomic reactor. Using UV-Vis spectroscopy methods, changes in the throughput of ceramics were evaluated depending on the irradiation fluence and the energy of incident ions. It was found that a change in the irradiation conditions leads to the formation of irradiation-induced defects with an energy of 2.4-2.45 eV in the structure, the concentration of which increases with the irradiation dose. Changes in the band gap and refractive index depending on irradiation fluence and incident ions energy indicate a change in the electronic and optical density of ceramics, as well as the formation of additional absorbing centers in the structure.
Key words: swift heavy ion, optical properties, absorbance, defects, ZrO_2 ceramic, irradiation

Introduction

На сегодняшний день оксидные диэлектрические керамики или наноструктурные оксидные керамики являются одними из перспективных классов материалов для широкого спектра применения их в практическом применении. Интерес к ним обусловлен их физико-химическими свойствами, а также высокими показателями устойчивости к внешним воздействиям, а также различным модификациям, которые открывают широкие перспективы для применения их в различных отраслях промышленности, включая энергетику [1-8]. При этом отдельное внимание среди исследователей уделяется изучению как способов получения оксидных керамик, так и изучения влияния на них внешних воздействий, коррозионных процессов, а также радиационных повреждений.

One of the important directions in modern materials science and energy is the study of the behavior of structural and optical changes in dielectric ceramics arising under external influences, such as corrosion, exposure to aggressive media, radiation exposure [9-14]. The study of such processes plays a highly important role in determination of performance characteristics of materials, as well as their resistance to external influences. At the same time, both theoretical research and experimental data are important in these studies, which allow developing not only the foundations of studying the properties of materials and the dynamics of their change, but also to obtain practical knowledge necessary for the design and application of materials in industry [15-19].

The most important area of research in the study of the influence of external factors is the study of the radiation damage effect on physicochemical properties of dielectric ceramics, which arise when they interact with ionizing radiation [20-21]. In case of irradiation of structural materials or ceramics with different types of ionizing radiation, processes of radiation interaction with crystalline structure of materials have multi-stage and complex character, including primary and secondary processes of radiation interaction with matter [22,23]. The final stage of primary processes is ionization and the formation of primary knocked-out atoms, which entail a change in electron density in the material. Secondary processes, in turn, lead to the formation of point defects, vacancies, and disordering regions at high irradiation fluences. It is important to note here that the final evolution of both primary and secondary processes has a direct dependence on the irradiation fluences and the formed defective regions [24-26]. For example, with small irradiation fluences, defective regions in dielectric ceramics are isolated from each other, resulting in the formation of single defects and a low disordering degree, which in most cases do not significantly affect the change in material properties. At high irradiation fluences, which are characterized by the formation of defect overlap regions, these disordering regions and point defects are not isolated from each other and, therefore, make a collective contribution to the change in the properties of materials, which can be catastrophic in some cases. It should be noted that, according to various estimates, the boundary of defect regions overlapping onset varies from 10^{12} to 10^{14} ion/cm^2, depending on the type of incident ions and their energies [27,28]. In turn, depending on the class of materials, the final evolution of radiation damage also has significant differences, which leads to the inadmissibility of applying a unified theory to describe all the observed effects and gives rise to a large number of different theoretical interpretations of radiation defects in materials. In particular, for ceramics, the theory most commonly used to describe radiation damage is the theory of the formation of so-called thermal bursts or thermal peaks arising along the trajectory of an incident particle, which are accompanied by the appearance of local temperature gradients comparable to the plasma temperature [29-31]. The formation of such local regions results in a large number of small point defects capable of making significant changes in the properties of materials, up to the formation of radiation damage, called latent tracks or disordering regions [32,33]. Moreover, if for metals the occurrence and subsequent evolution of radiation damage is well described and has a large number of experimental evidence of the proposed theoretical research, then for ceramics, in particular zirconia, such data are quite small, despite the great interest in this class of ceramics, both from a fundamental and practical point of view.

As is known, ceramics based on zirconium dioxide are one of the promising classes of ionic conductors that have found wide application in various technological applications, as well as in nuclear power [34-38]. Как известно из ранее проведенных исследований, керамики на оксида циркония, а также различные их модификации обладают уникальными оптическими свойствами, которые позволяют использовать их в широком спектре практических применений [39-42]. In this case, the previously established processes of phase transformations [43] under the action of irradiation in ZrO_2 ceramic open up a large number of questions concerning the effect of irradiation not only on the structural properties of ceramics, but also on optical characteristics, since this type of ceramics has great potential for use as a basis for optical devices capable of operating in conditions of increased radiation background, including in the core of nuclear reactors.

Based on the foregoing, the aim of this work is to study the effect of irradiation with heavy ions Xe^{22+} with energies of 165 MeV, 200 MeV, and 230 MeV on the change in the optical properties of ZrO_2 ceramic. The choice of ion energies, as well as radiation fluences of 10^{13}-10^{14} ion/cm^2, is primarily due to the possibility of simulating radiation damage in ceramics that occurs when overlapping damaged areas in the material, comparable to damage from fission fragments of uranium nuclei in an atomic reactor.

Experimental part

The initial samples were polycrystalline ZrO_2 ceramics with a tetragonal crystal lattice and spatial system P42/nmc(137).

The initial polycrystalline ZrO_2 ceramic samples were irradiated with heavy Xe^{22+} ions with energies of 165 MeV, 200 MeV, and 230 MeV and fluences of 10^{13}-10^{14} ion/cm^2. The choice of radiation doses is due to the possibility of simulating the effects of radiation damage and the initialization of gas swelling processes under irradiation with uranium fission fragments. According to calculated data, the concentration of implanted Xe^{22+} ions in the structure of ceramics is 0.001-0.01 at.%. In view of the large atomic radius and low mobility of implanted Xe^{22+} ions, the final stage of evolution is the formation of gas-filled bubbles in the near-surface layer. The formation of such bubbles leads to a decrease in mechanical, heat-conducting, strength properties, as well as optical characteristics.

The irradiation of samples was carried out on a DC-60 heavy ion accelerator, on the third channel designed to simulate radiation damage by various types of ions in a wide energy range. The samples were placed in a special target holder cooled with water in order to avoid heating the samples during irradiation. The temperature of the samples during irradiation was no more than 50-70°C.

Determination of the radiation effect and the consequences of radiation damage on the change in optical properties, as well as the change in optical and electron density were carried out using optical UV-Vis spectroscopy, by taking UV-Vis spectra in the wavelength range from 300 to 800 nm, with a step of 1 nm.

Determination of the induced absorption value was carried out by logarithm of the ratio of the transmission spectra. The absorption value characterizing the change in optical and electron density was estimated by changing the transmission spectra and the shift of the fundamental absorption edge.

The determination of the band gap and refractive index was carried out by making Tauc plots and subsequent analysis.

Results and discussion

Figure 1 shows the results of measuring the optical transmission spectra of the studied ZrO_2 ceramic depending on the energy and fluence of incident ions. In this section, the UV-Vis spectra are grouped as a dependence of the increase in the radiation dose at one ion energy. This grouping is due to the need to show changes in optical transmission spectra depending on an increase in radiation damage degree at the same energy of incident ions. The initial transmission spectrum of ZrO_2 ceramic is characterized by a fundamental absorption edge in the region of 320-350 nm, as well as high transmission rates in a wide wavelength range. The main nature of the change in optical properties depending on the radiation dose is primarily associated with a shift in the fundamental absorption edge, as well as a sharp drop in the transmission value in the region of 400-600 nm.

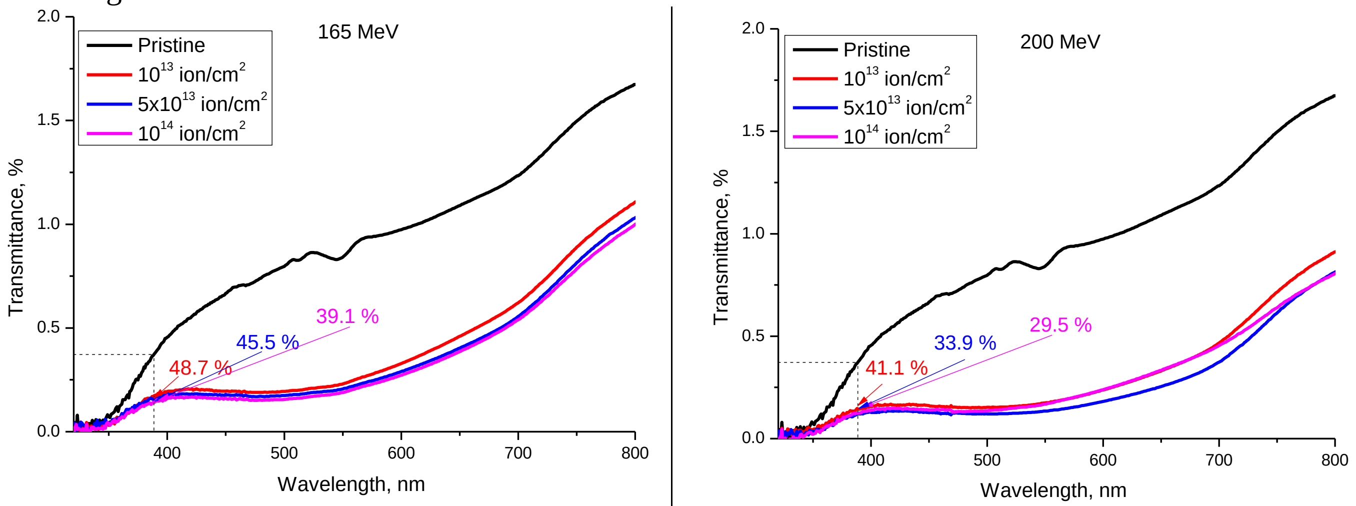

a) b)

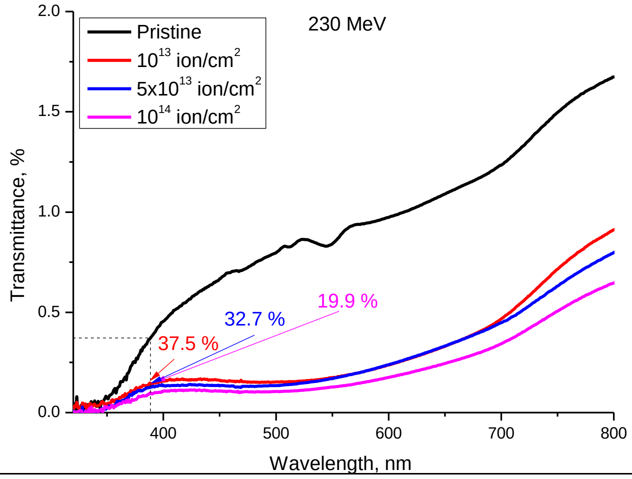

c)

Figure 1. UV-Vis transmission spectra of ZrO_2 ceramic before and after irradiation with heavy Xe^{22+} ions with various energies: a) 165 MeV; b) 200 MeV; c) 230 MeV

As can be seen from the data presented, a decrease in the transmission value in the range of 400-600 nm may be due to the formation of nanostructured inclusions or the fragmentation of grains with a metallic type of conductivity. Similar effects were observed when ZrO_2 ceramic were irradiated with ion irradiation [43-45]. Thus, the authors of these works have shown that when irradiated with low-energy ions with a large irradiation fluence, nanoinclusions are formed in the near-surface irradiated layer, which lead to the appearance of additional absorption centers and thereby reduce the transmission in this region. The formation of such inclusions, as shown by the authors of [43-45], leads to an increase in the absorption of light in this wavelength range. The very formation of such inclusions can be associated with the processes of knocking out zirconium ions from the sites of the crystal lattice and their subsequent coagulation, as well as rearrangement of the crystal lattice and its deformation. In this case, an increase in the energy of incident ions leads to more intense absorption in this region, which indicates an increase in the concentration of these absorbing centers and defects in the structure.

All obtained transmission variation dependences can be divided into two groups. The first group of changes is associated with an increase in irradiation fluence and is characterized by dependencies of a decrease in transmission with an increase in the irradiation fluence and, as is known, the concentration of radiation damage areas. In the case of energies of incident ions of 165 MeV, an increase in irradiation fluence from 10^{13} to $5x10^{13}$ ion/cm^2 leads to a reduction in transmission by 51.3 % and 54.5 %, respectively compared to the initial value. At the same time, the increase in fluence from 10^{13} to $5x10^{13}$ ion/cm^2 leads to a decrease in transmission by only 3.2 %, while a further increase in irradiation fluence up to 10^{14} ion/cm^2 leads to a decrease in the transmission by 60.9 % compared to the initial value of 9.6 % compared with the initial value and 9.6 % and 6.4 % compared to the similar transmission values for samples irradiated with doses of 10^{13} to $5x10^{13}$ ion/cm^2.

For samples irradiated with 200 MeV ions, the transmission decrease is more pronounced and is 58.9 %, 66.1 % and 70.5 % for irradiation fluences 10^{13}, $5x10^{13}$ and 10^{14} ion/cm^2, respectively. For samples irradiated with 230 MeV ions, a further decrease of 62.5 %, 67.3 % and 80.1 % for irradiation fluences 10^{13}, $5x10^{13}$ and 10^{14} ion/cm^2, respectively, is observed.

Such a decrease in transmittance is primarily due to large energy losses of the incident ions, which lead to an increase in the concentration of formed point defects, vacancies and primarily knocked out atoms, as well as an increase in the radius of the damage region. An increase in radiation damage areas along ion trajectories in the material while increasing the energy of the incident ions leads to an increase in overlapping degree of such regions and, therefore, more intense mixing of the formed point defects and vacancies. At the same time, an increase in irradiation fluence from $5x10^{13}$ ion/cm^2 to 10^{14} ion/cm^2, according to estimates given in the monograph [46], can lead to an increase in defective regions overlapping degree up to 100-1000 times. At the same time, according to [47] for ions with energies of more than 50 MeV, the predominance of electronic losses in the interaction of incident ions with a substance leads to the occurrence of local ionization, which causes further radiation damage. At the same time, as is known, the oxygen binding energy in the structure of ZrO_2 ceramic is much less than the zirconium binding energy, as a result of which the mobility of oxygen ions is much higher than that of zirconium ions, which leads to the formation of a large number of oxygen vacancies. Knocked out oxygen ions can migrate along the crystal lattice, and slow-moving zirconium ions can form additional defects, attaching electrons to themselves, thereby forming the nanoscale inclusions mentioned in works [43-45].

Such a similar behavior of the change in transmission value in the case of heavy ions is due to the fact that during irradiation, the energy losses of incident particles during elastic and inelastic interactions are several orders of magnitude higher than during low-energy irradiation, as a result of collisions, as well as primarily knocked out atoms in this case are much greater than during low-energy irradiation. It is worth to note that during high-energy irradiation, the interactions of incident ions with electron shells play an important role, which lead to the formation of a large number of knocked out electrons and, consequently, there is a change in the electron density near trajectories of ions in the material. In contrast to metals, for which relaxation processes play a significant role and after irradiation, most of the knocked out electrons return to their original positions, thereby compensating for changes in the electron density, for dielectrics such a process is extremely difficult, which can lead to the formation of regions with depleted or oversaturated electrons. The formation of such areas can lead to a change in the band gap, the results of which are shown in Figure 2.

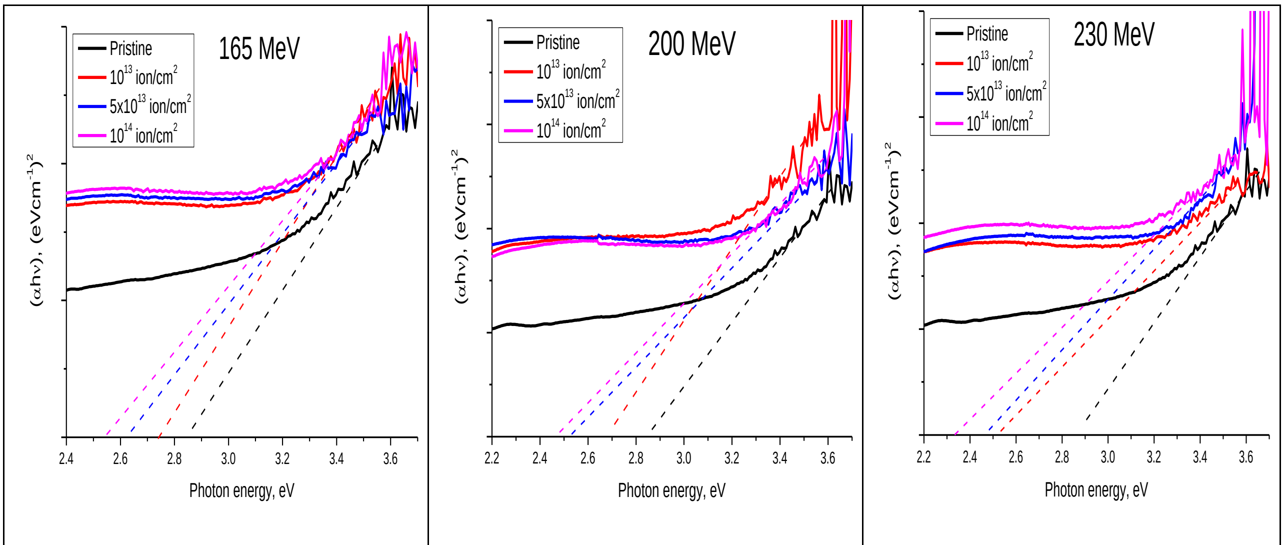

a)	b)	c)

Figure 2. Tauc plots a) 165 MeV; b) 200 MeV; c) 230 MeV

The general appearance of the band gap changes is related to the displacement of the fundamental absorption edge into the low energy region, which indicates a change in electron density and the formation of additional defects leading to absorption. Based on the obtained Tauc plots, the band gap and refractive index were determined, the data of which are shown in Table 1.
Определение величины ширины запрещенной зоны проводилось с использованием формулы (1):

$$\alpha = A(h\nu - E_g)^{1/2}, \qquad (1)$$

where *A* is a constant and *hν* is the photon energy.
Определение коэффициента преломления было проведено с использованием следующей формулы (2):

$$\left[\frac{(n^{optical})^2 - 1}{(n^{optical})^2 + 2}\right] = 1 - \sqrt{\frac{E_g}{20}}, \quad (2)$$

где E_g – ширина запрещенной зоны.

Table 1. Data on changes in the values of the band gap and refractive index depending on the radiation dose

Fluence, ion/cm^2	Band gap, eV			
	Initial	165 MeV	200 MeV	230 MeV
10^{13}	2.85	2.74	2.68	2.63
$5x10^{13}$		2.62	2.54	2.46
10^{14}		2.55	2.47	2.34
Fluence, ion/cm^2	Refractive index			
	Initial	165 MeV	200 MeV	230 MeV
10^{13}	2.44	2.47	2.49	2.50
$5x10^{13}$		2.51	2.53	2.56
10^{14}		2.53	2.56	2.60

According to the obtained data, the largest changes in the band gap and refractive index are observed at large fluences and at maximum energies of incident ions. As mentioned above, such changes may be associated with changes in the optical density of the ceramics, the changes of which are directly dependent on radiation damage concentration and irradiation density. The formation of overlapping regions of damaged areas that occur along the ions movement trajectory in the material leads to the appearance of regions with an anisotropic distribution of electrons. At the same time, an increase in the energy of incident ions and the irradiation fluence leads to both an increase in the overlapping degree and an increase in the electron density distribution anisotropy. As previously shown, for dielectric materials, including polymers and ceramics, high-dose irradiation leads to the formation of crystal and electron anisotropy in the structure, which are expressed in a change in the diffraction maxima intensity with a circular scan of φ=0-360° [48,49], as well as the appearance of additional induced absorption bands, indicating a change in the electron density in the material [50]. Also, changes in the electron density can be associated with induced phase transformations of the t-ZrO_2 → c-ZrO_2 type in the structure of ZrO_2 ceramic under the action of irradiation with heavy ions [43].

An increase in the refractive index, in turn, characterizes an increase in the optical density, which is due to the formation of additional absorbing centers in the near-surface irradiated layer. As a rule, in dielectrics, the change in optical density (absorbance) depending on the irradiation fluence is characterized by a linear dependence, and the nature of linearity indicates the rate of increase in the concentration of defects and absorbing centers in the irradiated material. Figure 3a shows the results of change in absorbance depending on the energy of incident ions and irradiation fluence.

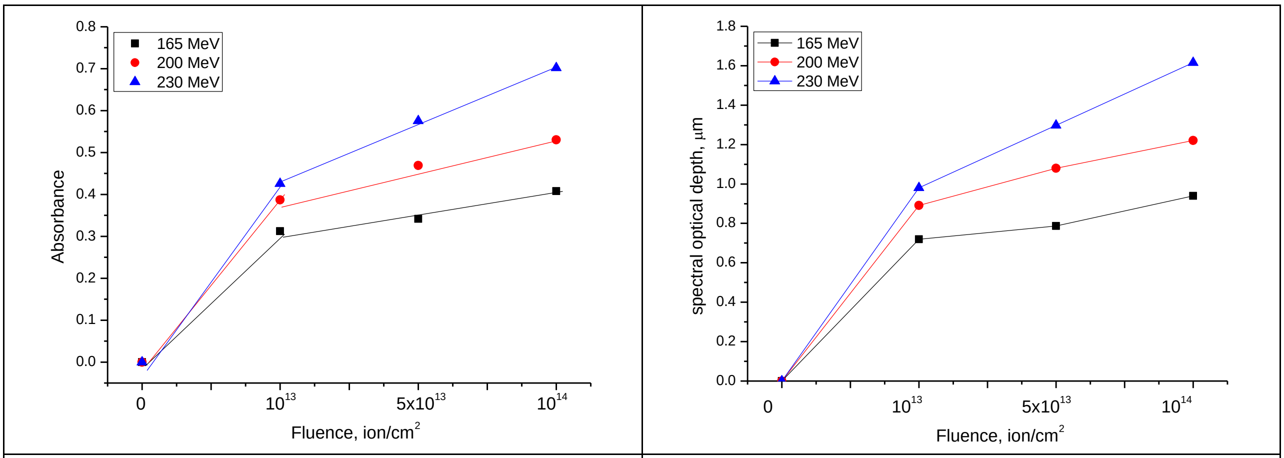

a) b)

Figure 3. a) Graph of the change in absorbance depending on irradiation fluence for Xe^{22+} ions of different energies; b) Graph of the change in optical depth of radiation damage induced by defects

As can be seen from the data presented, the obtained dependences of the change in the optical density have are in good agreement with the previously obtained data of linear dependences for irradiated materials. At the same time, an increase in the energy of incident ions from 165 MeV to 200 MeV does not affect the slope of the optical density change line, while irradiation with ions with an energy of 230 MeV leads to a sharp increase in the angle of inclination of the line, which indicates an increase in the defect formation rate in the irradiated material. In turn, an increase in optical density indicates an increase in the concentration of absorbing centers arising from irradiation. Applying a known expression that binds the optical density with the depth of radiation damage caused by irradiation and subsequent formation of defects, the dependence of change in depth of the lower concentration of optical defects caused by irradiation from the radiation dose and the energy of incident ions was constructed. The results of the constructions are presented in Figure 3b, according to which it can be seen that an increase in both the irradiation fluence and the energy of the incident ions leads to an increase in the thickness of the damaged layer with accumulated defects. An increase in optical density, as well as a layer depth with a modified optical density, can be due not only to radiation damage caused by the ionization processes and the subsequent formation of point and vacancy defects, but also to the formation of additional defects capable of forming additional absorbing centers. The formation of such centers can be associated both with the formed oxygen vacancies, as a result of knocked out oxygen from the crystal lattice nodes, and the formation of T-defects (zirconium ion + electron) arising from the breaking of chemical and crystalline bonds. In turn, the knocked out oxygen ions migrating to the surface create a large number of oxygen vacancies in the structure, and also create a positive charge gradient in the irradiated layer, which is compensated by the knocked out electrons. The charge compensation leads to the filling of a part of the energy levels in the band gap, which leads to its decrease. In this case, the formed T-defects will accumulate near the bottom of the conduction band due to the 4d-states of Zr, which form the valence band.

Figure 4 shows the results of determining changes in the induced absorption value, which was calculated by logarithm of the ratio of transmission spectra of ceramics in the initial and irradiated state. The difference spectrum in the energy representation reflects the formation of additional absorption bands in ceramics with a maximum of 2.4-2.45 eV, which corresponds to the formation energy of T-defects.

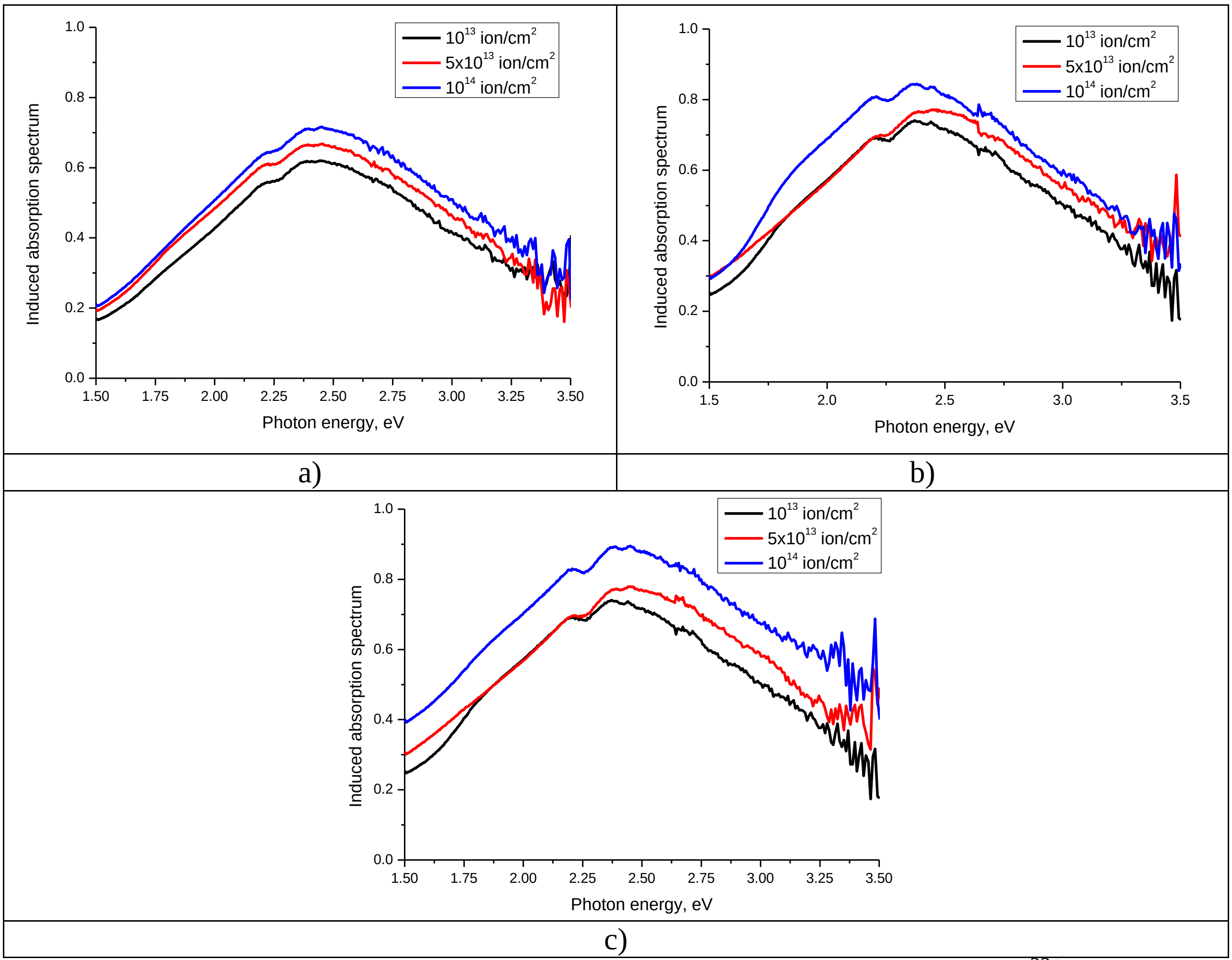

Figure 4. Graphs of the induced absorption in ceramics after irradiation with Xe^{22+} ions with different energies: a) 165 MeV; b) 200 MeV; c) 230 MeV

As can be seen from the data presented, an increase in the radiation dose leads to an increase in the induced absorption band intensity, which indicates an increase in the concentration of formed defects. At the same time, an increase in the ion energy to 200 and 230 MeV leads to the formation of double maxima, which indicates the formation of additional C-type defects associated with the formation of zirconium ions with two oxygen vacancies nearby. Evaluation of the induced absorption spectra maximum values (see Figure 5) indicates that an increase in the energy of incident ions from 200 to 230 MeV at irradiation doses of 10^{13}-$5x10^{13}$ ion/cm^2 leads to an insignificant increase in the concentration of induced defects, as compared to a similar value obtained from the analysis of the induced absorption spectra intensity of samples irradiated with an ion energy of 165 MeV.

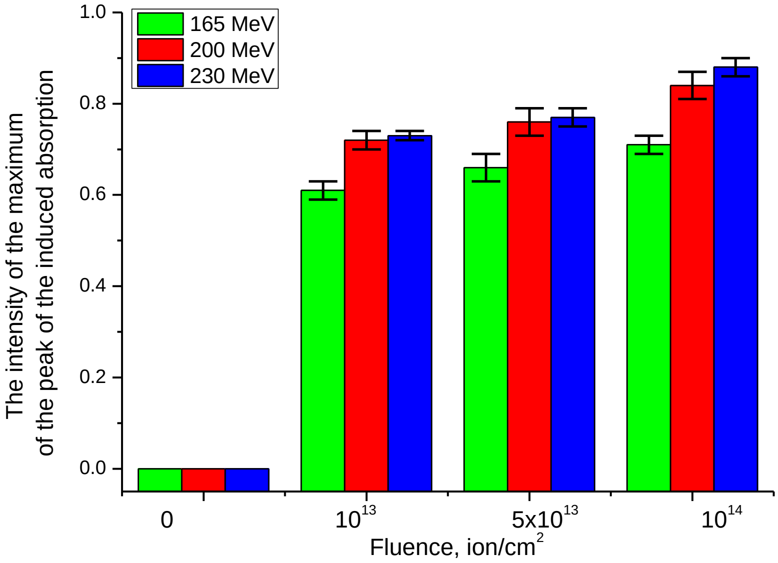

Figure 5. Diagram of the change in the induced absorption peak maximum, which characterizes the concentration of defects resulting from irradiation

The dependences of change in transmission spectra shown in Figure 6, grouped depending on the energy of incident ions at the same irradiation fluence, indicate that an increase in the energy of incident ions by an amount of 30-35 MeV leads to significant differences in the change in transmittance at doses of 10^{13}-$5x10^{13}$ ion/cm^2, which range from 1.2 to 7-12 % depending on the ion energy, while for samples irradiated at a fluence of 10^{14} ion/cm^2, the average decrease in transmittance is 10 % with an increase in the energy of ions. Such differences may be due to a change in the probability of overlapping defective regions, which for fluence 10^{13}-$5x10^{13}$ ion/cm^2 is 10-50 times the overlap, according to estimates [46], and has a pronounced dependence on the radii of these regions. According to estimates from earlier studies, the radius of this region can vary from 3 to 10 nm depending on the energy of the incident particles. At the same time, the radius of the region with the changed electron density, according to some estimates, can significantly exceed these dimensions, depending on the energy of the particles [51]. While for irradiation fluence of 10^{14} ion/cm^2, this value is much larger, and thus the dependence on the radius of the damaged area becomes not as significant as for small fluences.

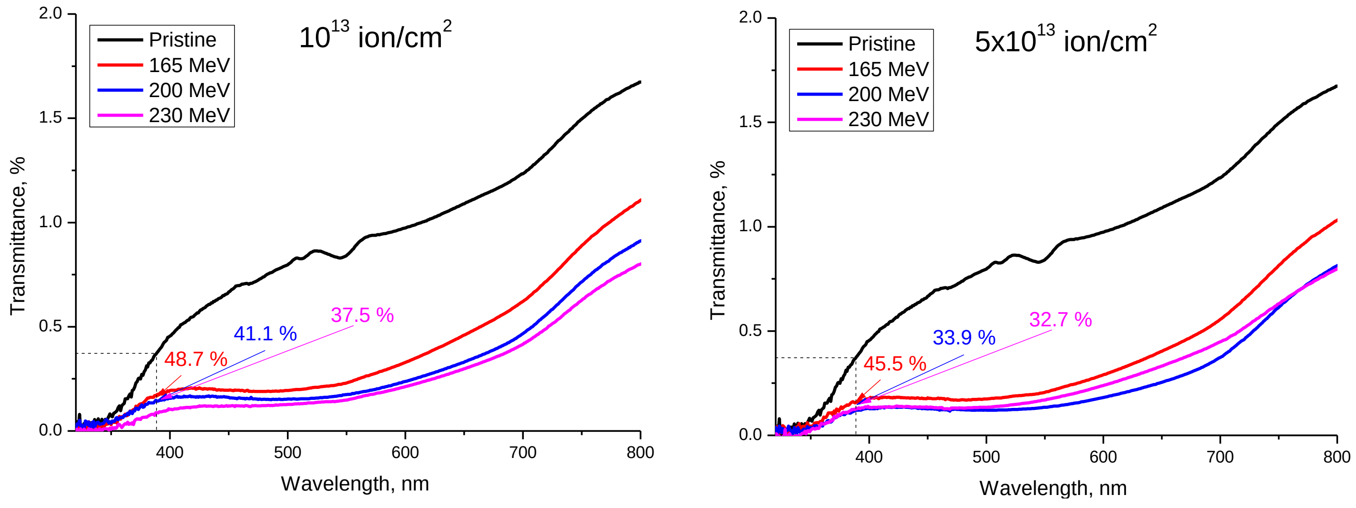

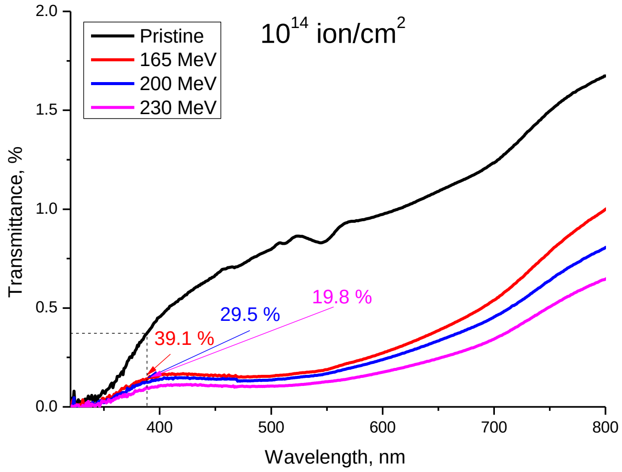

c)

Figure 6. UV-Vis transmission spectra of ZrO_2 ceramics before and after irradiation with heavy Xe^{22+} ions, depending on the energy of incident particles (the spectra are grouped by dose): a) 10^{13} ion/cm^2; b) $5x10^{13}$ ion/cm^2; c) 10^{14} ion/cm^2

Conclusion

The paper presents the results of a study of the effect of Xe^{22+} heavy ion irradiation on the optical properties of ZrO_2 ceramic. The study of optical characteristics was carried out using the UV-Vis spectroscopy, which allows assessing with high accuracy the change in transmission, band gap, refractive index and induced absorption without destroying the samples. The obtained dependences of changes in optical properties of ZrO_2 ceramic characterize the effect of radiation damage in a wide energy and dose range. В ходе проведенных исследований было установлено, что увеличение энергии налетающих ионов на величину 30-35 МэВ, приводит к существенным различиям в изменении величины пропускания при дозах 10^{13}-$5x10^{13}$ ион/см^2, которые варьируются от 1.2 до 7-12 % в зависимости от энергии ионов, в то время как для образцов облученных при флюенсе 10^{14} ион/см^2 среднее уменьшение величины пропускания составляет 10 % с увеличением энергии ионов.

The established dose and energy dependences of the induced absorption bands formation, as well as changes in the band gap and transmission, made it possible to estimate the change in the electron and optical density of ceramics before and after irradiation.

In the future, dependences obtained can serve to expand the fundamental knowledge about the dynamics of radiation damage in ZrO_2 ceramic, and can also be used as a basis for determination of the service life of these ceramics as optoelectronic devices exposed to radiation effects comparable in energy to uranium fission fragments.

Funding

This work was supported by the Grant No. BR09158499 (Development of complex scientific research in the field of nuclear and radiation physics on the basis of Kazakhstan accelerator complexes) of the Ministry of Energy of the Republic of Kazakhstan.

Compliance with Ethical Standards

Conflict of Interest: The authors declare that they have no conflict of interest.

Ethical approval: This chapter does not contain any studies with human participants or animals performed by any of the authors.

Informed consent: Informed consent was obtained from all individual participants included in the study.

References

1 Batoo, Khalid Mujasam, et al. "Improved room temperature dielectric properties of Gd3+ and Nb5+ co-doped Barium Titanate ceramics." Journal of Alloys and Compounds (2021): 160836.
2 Prakash, Deo, et al. "Synthesis, purification and microstructural characterization of nickel doped carbon nanotubes for spintronic applications." Ceramics International 42.5 (2016): 5600-5606.
3 Rais, A., et al. "Copper substitution effect on the structural properties of nickel ferrites." Ceramics International 40.9 (2014): 14413-14419.
4 Al-Gaashani, R., et al. "XPS and optical studies of different morphologies of ZnO nanostructures prepared by microwave methods." Ceramics International 39.3 (2013): 2283-2292.
5 Al-Douri, Y., et al. "Detecting the DNA of dengue serotype 2 using aluminium nanoparticle doped zinc oxide nanostructure: synthesis, analysis and characterization." Journal of Materials Research and Technology 9.3 (2020): 5515-5523.
5 Bouhemadou, Abdelmadjid, et al. "Electronic, optical, elastic, thermoelectric and thermodynamic properties of the spinel oxides ZnRh2O4 and CdRh2O4." Journal of Alloys and Compounds 774 (2019): 299-314.
6 Monir, Mohammed El Amine, et al. "Doping-induced half-metallic ferromagnetism in vanadium and chromium-doped alkali oxides K 2 O and Rb 2 O: Ab initio method." Journal of Superconductivity and Novel Magnetism 30.8 (2017): 2197-2210.
7 Bouhemadou, A., et al. "Structural, elastic, electronic, chemical bonding and optical properties of Cu-based oxides ACuO (A= Li, Na, K and Rb): An ab initio study." Computational materials science 81 (2014): 561-574.
8 Xu, Tianzhao, et al. "Anti-corrosion LaO3/2-GaO3/2-ZrO2 infrared glasses with high refractive index and low dispersion prepared by aerodynamic levitation." Optical Materials 114 (2021): 110943.
9 Naser, M. Z. "Properties and material models for common construction materials at elevated temperatures." Construction and Building Materials 215 (2019): 192-206.
10 Björk, Folke, and Tomas Enochsson. "Properties of thermal insulation materials during extreme environment changes." Construction and Building Materials 23.6 (2009): 2189-2195.
11 Mustafin, E., et al. "Ion irradiation studies of construction materials for high-power accelerators." Radiation Effects & Defects in Solids 164.7-8 (2009): 460-469.
12 Uvarov, V. T., et al. "Radiation-acoustic control over the thermal parameter of construction materials irradiated by intense relativistic electron beams." Physics of Particles and Nuclei Letters 11.3 (2014): 274-281.
13 Byun, T. S., and K. Farrell. "Tensile properties of Inconel 718 after low temperature neutron irradiation." Journal of Nuclear Materials 318 (2003): 292-299.
14 Chin, Joannie W., Tihn Nguyen, and Khaled Aouadi. "Effects of environmental exposure on fiber-reinforced plastic (FRP) materials used in construction." Journal of Composites, Technology and Research 19.4 (1997): 205-213.
15 Zinkle, S. J., and E. R. Hodgson. "Radiation-induced changes in the physical properties of ceramic materials." Journal of nuclear materials 191 (1992): 58-66.
16 Kadyrzhanov, K. K., K. Tinishbaeva, and V. V. Uglov. "Investigation of the effect of exposure to heavy Xe22+ ions on the mechanical properties of carbide ceramics." Eurasian Phys. Tech. J 17 (2020): 46-53.
17 Mirzayev, M. N., et al. "Crystal structure changes and weight kinetics of silicon-hexaboride under gamma irradiation dose." Results in Physics 10 (2018): 541-545.
18 Snead, L. L., S. J. Zinkle, and D. P. White. "Thermal conductivity degradation of ceramic materials due to low temperature, low dose neutron irradiation." Journal of nuclear materials 340.2-3 (2005): 187-202.
19 Johnson, Carl E., K. R. Kummerer, and E. Roth. "Ceramic breeder materials." Journal of Nuclear Materials 155 (1988): 188-201.

20 Wang, Fei, et al. "Irradiation damage in (Zr0. 25Ta0. 25Nb0. 25Ti0. 25) C high-entropy carbide ceramics." Acta Materialia 195 (2020): 739-749.
21 Florez, Raul, et al. "The irradiation response of ZrC ceramics under 10 MeV Au3+ ion irradiation at 800 ºC." Journal of the European Ceramic Society 40.5 (2020): 1791-1800.
22 Han, Aifang, et al. "Prolonged UV-C irradiation is a double-edged sword on the zirconia surface." ACS omega 5.10 (2020): 5126-5133.
23 Stepanov, Vladimir A., Pavel V. Demenkov, and Olga V. Nikulina. "Radiation hardening and optical properties of materials based on SiO2." Nuclear Energy and Technology 7 (2021): 145.
24 Naik, R., et al. "Linear and nonlinear optical properties change in Ag/GeS heterostructure thin films by thermal annealing and laser irradiation." Optical and Quantum Electronics 52.3 (2020): 1-18.
25 Yamamoto, Yuki, et al. "Analysis of Ion-Irradiation Induced Lattice Expansion and Ferromagnetic State in CeO2 by Using Poisson Distribution Function." Quantum Beam Science 4.3 (2020): 26.
26 Lang, Maik, et al. "Fundamental Phenomena and Applications of Swift Heavy Ion Irradiations." arXiv preprint arXiv:2001.03711 (2020).
27 Rymzhanov, R. A., N. Medvedev, and A. E. Volkov. "Damage threshold and structure of swift heavy ion tracks in Al2O3." Journal of Physics D: Applied Physics 50.47 (2017): 475301.
28 Rymzhanov, R. A., et al. "Recrystallization as the governing mechanism of ion track formation." Scientific reports 9.1 (2019): 1-10.
29 Han, Xinqing, et al. "Latent Tracks in Ion-Irradiated LiTaO3 Crystals: Damage Morphology Characterization and Thermal Spike Analysis." Crystals 10.10 (2020): 877.
30 Mieskes, H. D., et al. "Electronic and nuclear thermal spike effects in sputtering of metals with energetic heavy ions." Physical Review B 67.15 (2003): 155414.
31 Wang, Z. G., et al. "Electronic thermal spike effects in intermixing of bilayers induced by swift heavy ions." Nuclear Instruments and Methods in Physics Research Section B: Beam Interactions with Materials and Atoms 209 (2003): 194-199.
32 Amekura, H., et al. "Ion tracks in silicon formed by much lower energy deposition than the track formation threshold." Scientific reports 11.1 (2021): 1-11.
33 Tomić Luketić, Kristina, et al. "Investigation of Ion Irradiation Effects in Silicon and Graphite Produced by 23 MeV I Beam." Materials 14.8 (2021): 1904.
34 Sathyaseelan, B., et al. "Studies on structural and optical properties of ZrO2 nanopowder for opto-electronic applications." Journal of Alloys and Compounds 694 (2017): 556-559.
35 Peuchert, Ulrich, et al. "Transparent cubic-ZrO2 ceramics for application as optical lenses." Journal of the European Ceramic Society 29.2 (2009): 283-291.
36 Guo, Hanzheng, et al. "Current progress and perspectives of applying cold sintering process to ZrO2-based ceramics." Scripta Materialia 136 (2017): 141-148.
37 Sabur, Abdus, et al. "Investigation of material removal characteristics in EDM of nonconductive ZrO2 ceramic." Procedia Engineering 56 (2013): 696-701.
38 Börner, Floriana-Dana, Wolfgang Lippmann, and Antonio Hurtado. "Laser-joined Al2O3 and ZrO2 ceramics for high-temperature applications." Journal of nuclear materials 405.1 (2010): 1-8.
39 Chen, Penghui, et al. "Influence of terminal pH value on co-precipitated nanopowders for yttria-stabilized ZrO2 transparent ceramics." Optical Materials 98 (2019): 109475.
40 Hou, Xiaorui, et al. "Effect of ZrO2 on the sinterability and spectral properties of (Yb0. 05Y0. 95) 2O3 transparent ceramic." Optical Materials 32.9 (2010): 920-923.
41 Gan, Lin, et al. "The effects of the temperature and pressure on ZrO2-doped transparent yttria ceramics fabricated by a hot-pressing method." Optical Materials 71 (2017): 109-116.
42 Wang, Shu Fen, et al. "Structure evolution and photoluminescence properties of ZrO2: Eu3+ nanocrystals." Optical materials 28.10 (2006): 1222-1226.
43 Alin, M., et al. "Comprehensive study of changes in the optical, structural and strength properties of ZrO2 ceramics as a result of phase transformations caused by irradiation with heavy ions." Journal of Materials Science: Materials in Electronics (2021): 1-12.

43 Gorshkov, Oleg N., et al. "Fabrication of the nanocrystal structures ZrO2 (y): Zr and SiO2: Si (p) by ion implantation." International Workshop on Nondestructive Testing and Computer Simulations in Science and Engineering. Vol. 3687. International Society for Optics and Photonics, 1999.,
44 Gorshkov, O. N., V. A. Novikov, and A. P. Kasatkin. "Formation of nanoparticles in the surface layer of stabilized ZrO 2 under ion irradiation." Neorganicheskie Materialy 35.5 (1999): 604-610.
45 Saito, Y., Y. Imamura, and A. Kitahara. "Optical properties of YSZ implanted with Ag ions." Nuclear Instruments and Methods in Physics Research Section B: Beam Interactions With Materials and Atoms 206 (2003): 272-276.
46 Wesch, Werner, and Elke Wendler. Ion beam modification of solids. Vol. 61. Springer Nature, 2016.
47 Weber, William J., et al. "The role of electronic energy loss in ion beam modification of materials." Current Opinion in Solid State and Materials Science 19.1 (2015): 1-11.
48 Kozlovskiy A.L. et. al. Study of the radiation disordering mechanisms of AlN ceramic structure as a result of helium swelling Journal of Materials Science: Materials in Electronics (2021) doi10.1007/s10854-021-06684-x
49 Tuleushev, Adil Z., et al. "Induced spirals in polyethylene terephthalate films irradiated with ar ions with an energy of 70 MeV." Crystals 10.6 (2020): 427.
50 Tuleushev, Adil Z., et al. "Assessment of the Irradiation Exposure of PET Film with Swift Heavy Ions Using the Interference-Free Transmission UV-Vis Transmission Spectra." Polymers 13.3 (2021): 358.
51 Enculescu, M., et al. "Heavy ion induced damage in NaCl and KCl crystals." Nuclear Instruments and Methods in Physics Research Section B: Beam Interactions with Materials and Atoms 229.3-4 (2005): 397-405.